Supporting Information

Axial Coordination Engineering for Single-Atom Catalysts in Bifunctional Oxidation NO and Mercury

Jianghao Cai [a, b], Tongao Yao [a, b], Haoqi Tian [a, b], XiaoTian Tang [a, b], Yutong Jiang [a, b], Ruiyang Shi [a, b], Binghui Zhou [a, b], Zhengyang Gao [a, b], Weijie Yang [a, b, *]

a Department of Power Engineering, School of Energy, Power and Mechanical Engineering, North China Electric Power University, Baoding, 071003, China

b Hebei Key Laboratory of Low Carbon and High Efficiency Power Generation Technology, North China Electric Power University, Baoding, 071003, Hebei, China

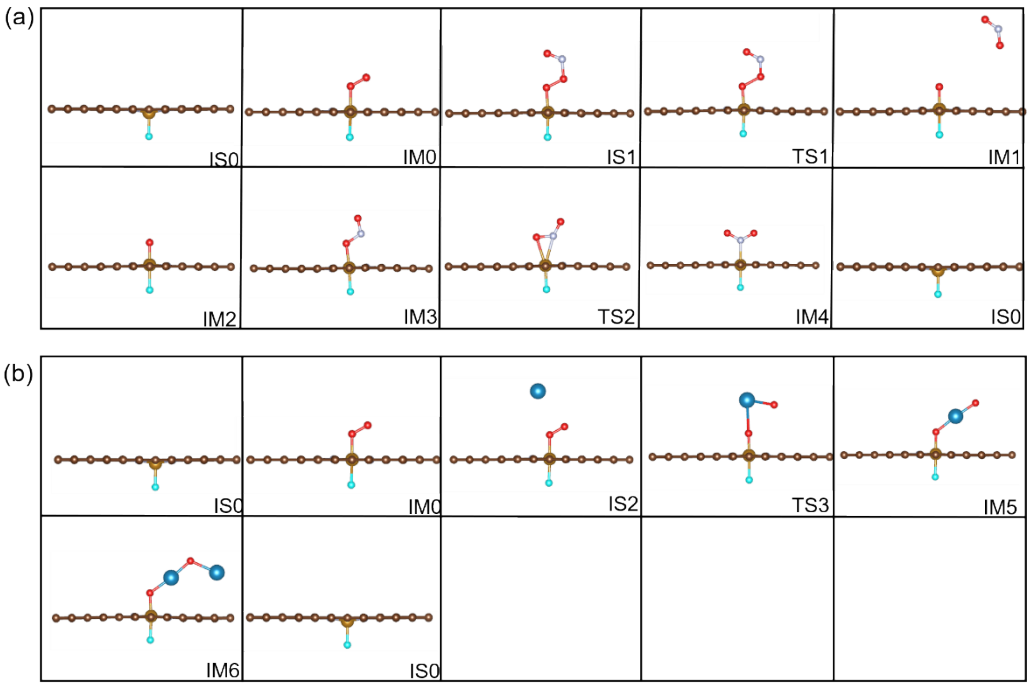

Figure S1. (a) Oxidation pathway of NO on Fe_1N_4-F. (b) Oxidation pathway of Hg^0 on Fe_1N_4-F.

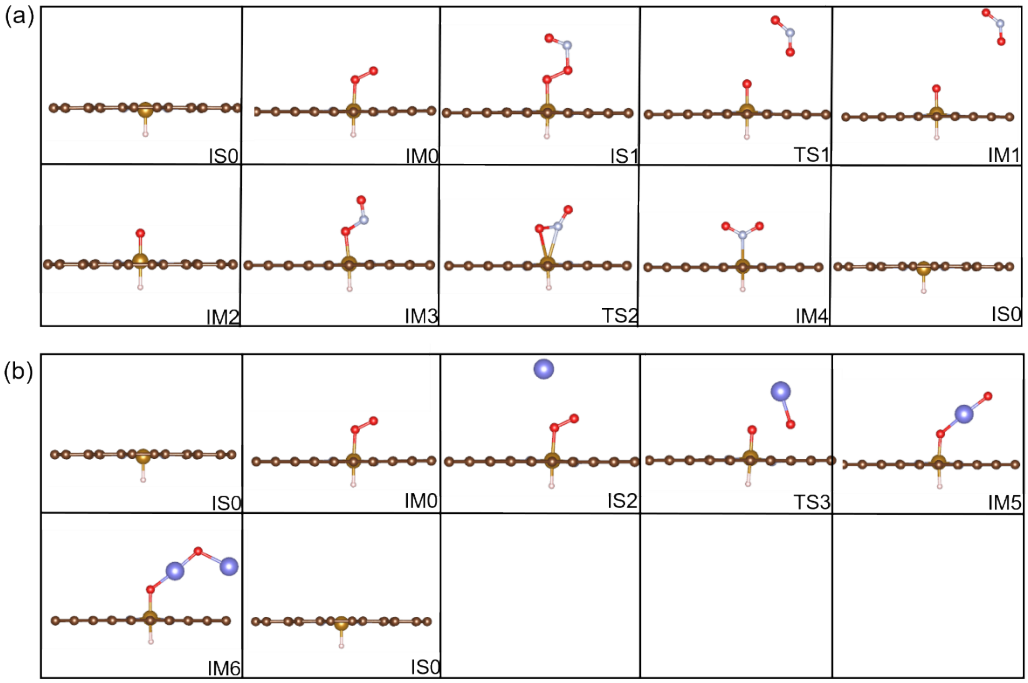

Figure S2. (a) Oxidation pathway of NO on Fe_1N_4-H. (b) Oxidation pathway of Hg^0 on Fe_1N_4- H.

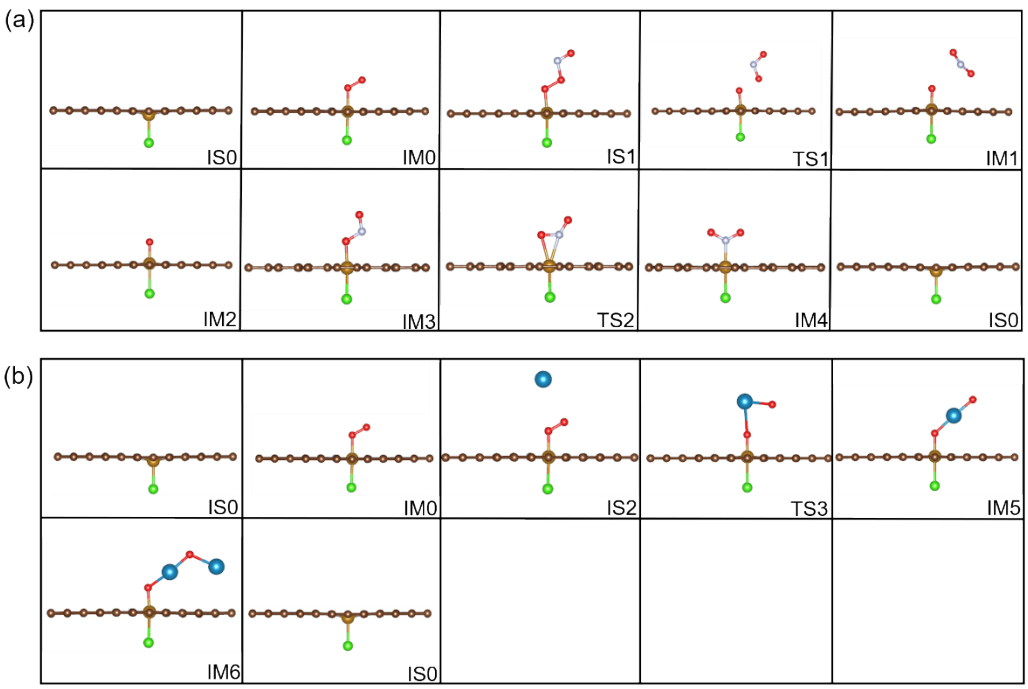

Figure S3. (a) Oxidation pathway of NO on Fe_1N_4-Cl. (b) Oxidation pathway of Hg^0 on Fe_1N_4-Cl.

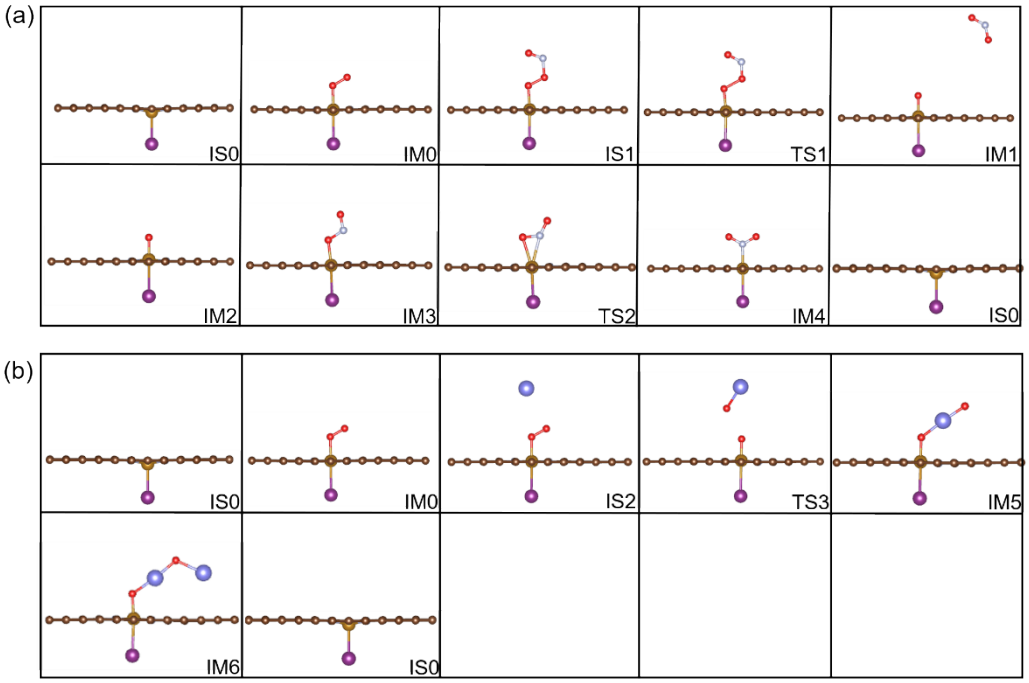

Figure S4. (a) Oxidation pathway of NO on Fe_1N_4-I. (b) Oxidation pathway of Hg^0 on Fe_1N_4-I.

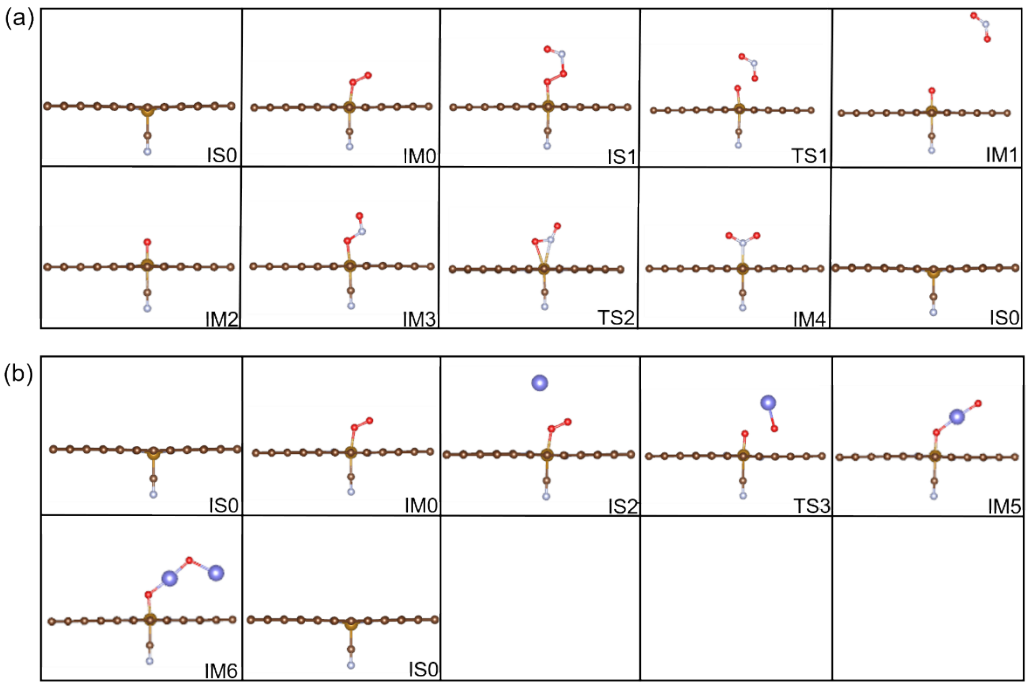

Figure S5. (a) Oxidation pathway of NO on Fe_1N_4-CN. (b) Oxidation pathway of Hg^0 on Fe_1N_4-CN.

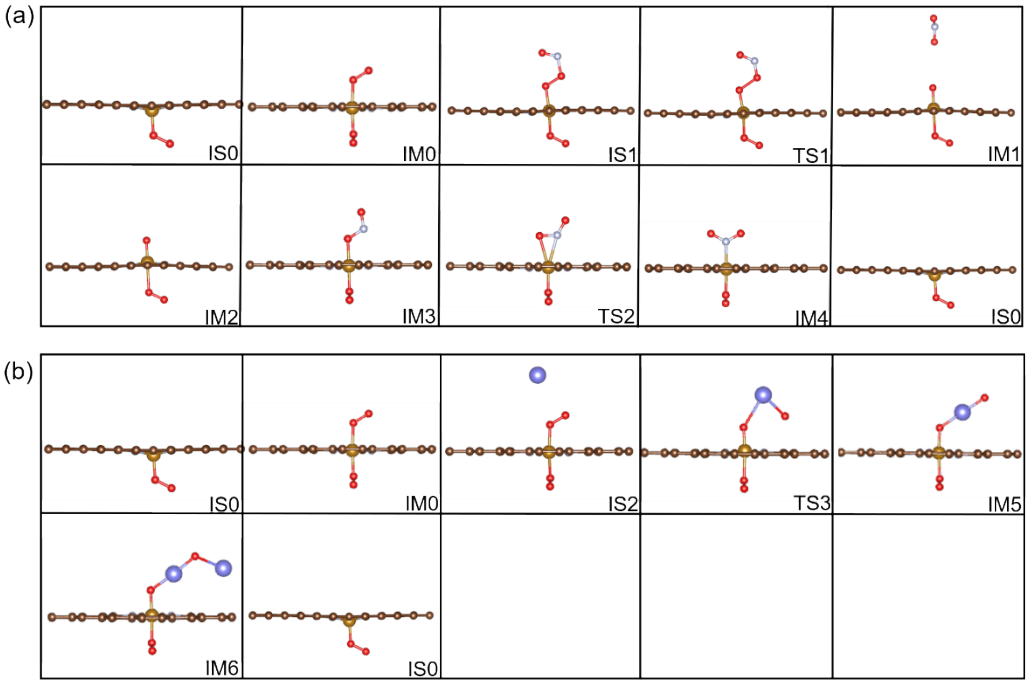

Figure S6. (a) Oxidation pathway of NO on Fe_1N_4-O_2. (b) Oxidation pathway of Hg^0 on Fe_1N_4-O_2.

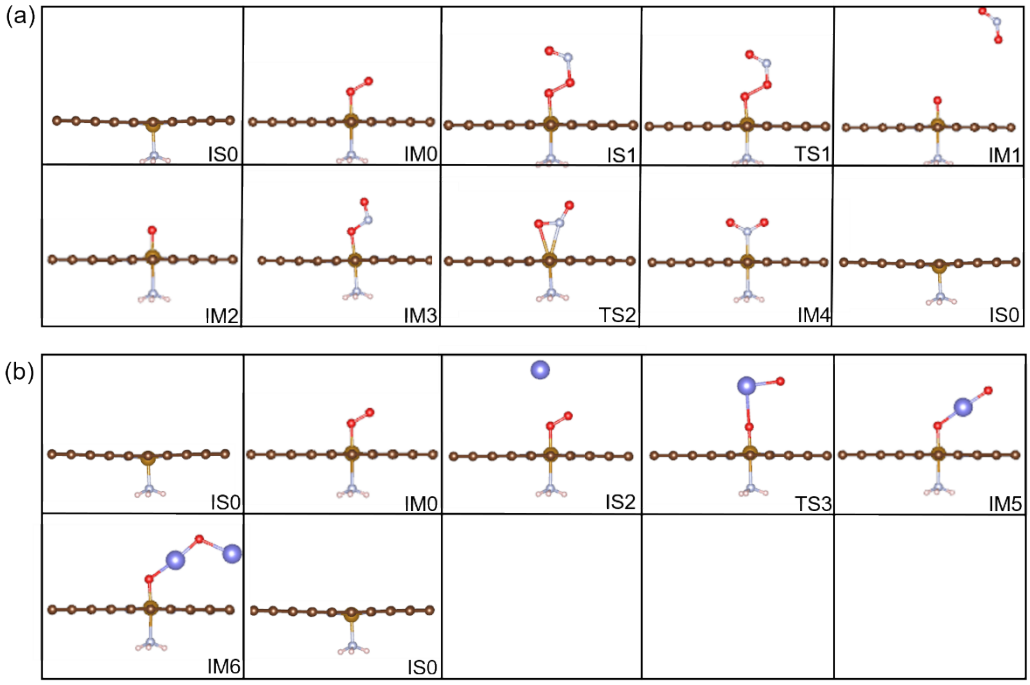

Figure S7. (a) Oxidation pathway of NO on Fe_1N_4-NH_3. (b) Oxidation pathway of Hg^0 on Fe_1N_4-NH_3.

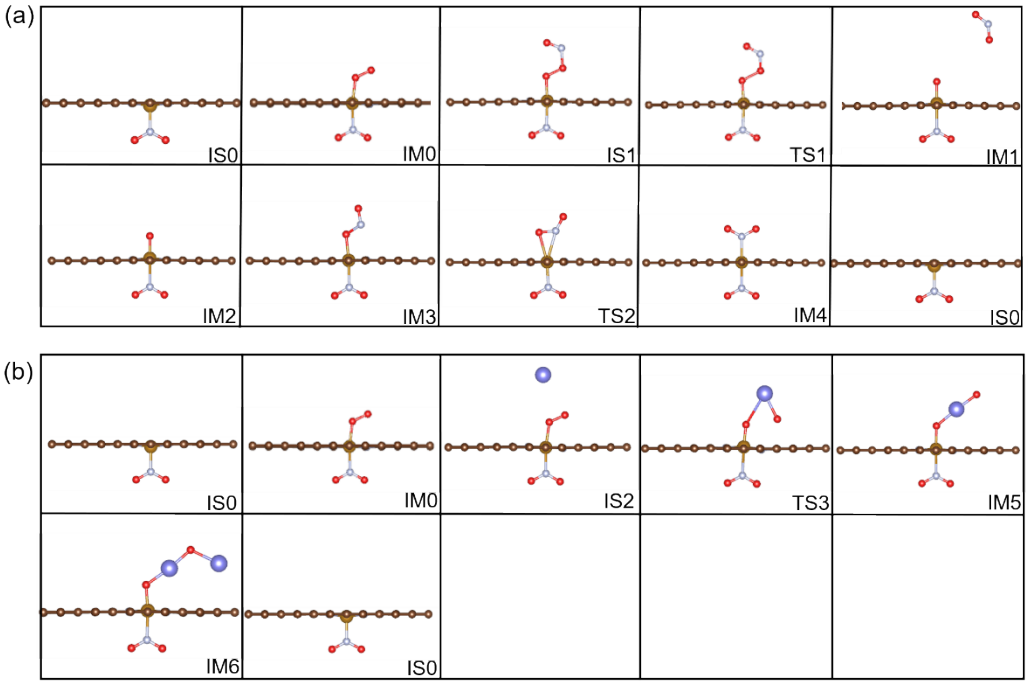

Figure S8. (a) Oxidation pathway of NO on Fe_1N_4-NO_2. (b) Oxidation pathway of Hg^0 on Fe_1N_4-NO_2.

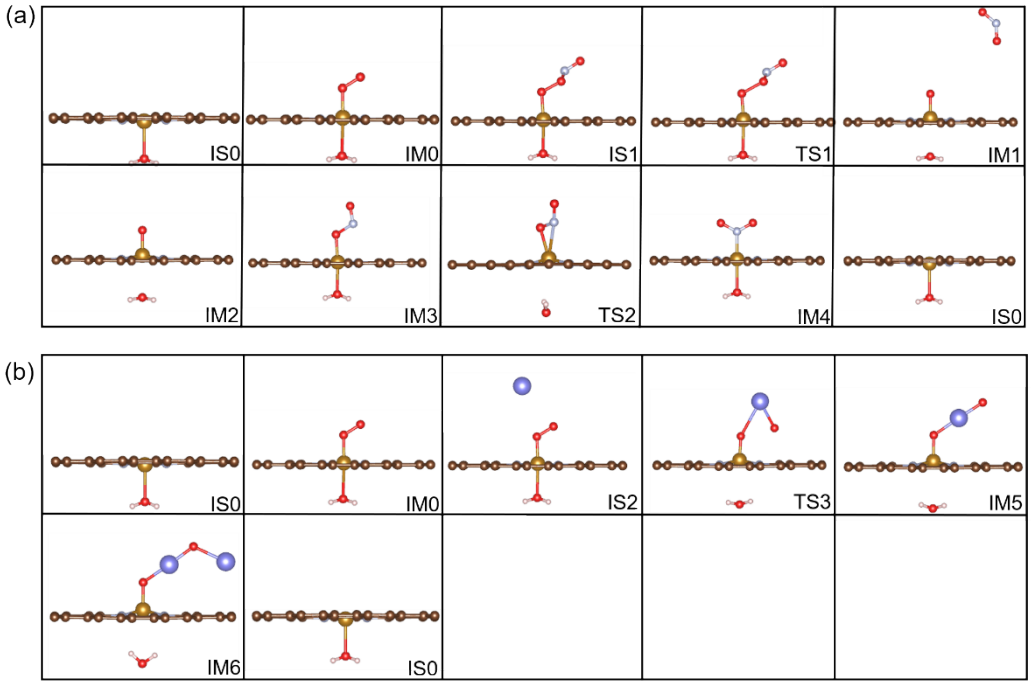

Figure S9. (a) Oxidation pathway of NO on Fe_1N_4-H_2O. (b) Oxidation pathway of Hg^0 on Fe_1N_4-H_2O.

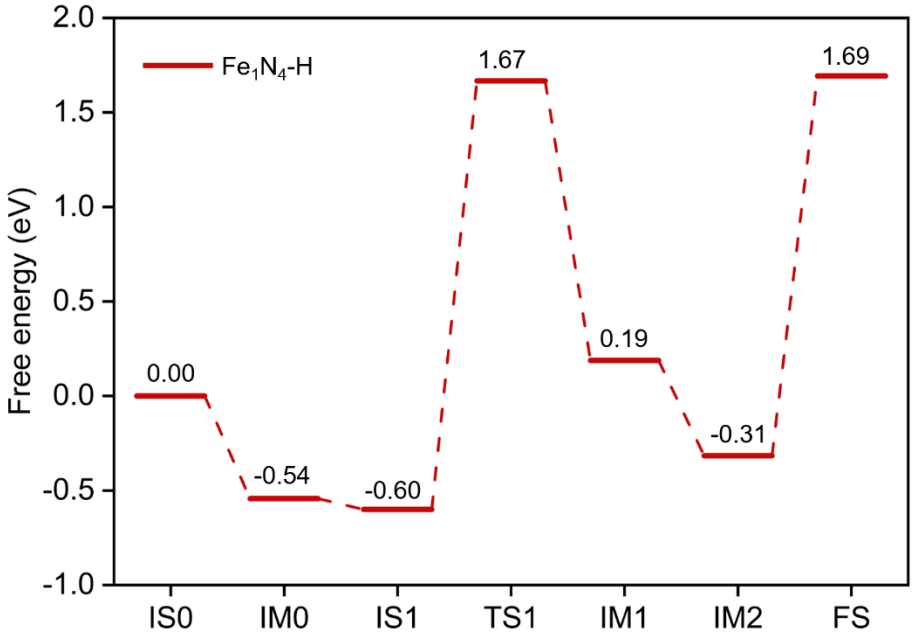

Figure S10. Free energy diagram of NO oxidation on Fe_1N_4-H.

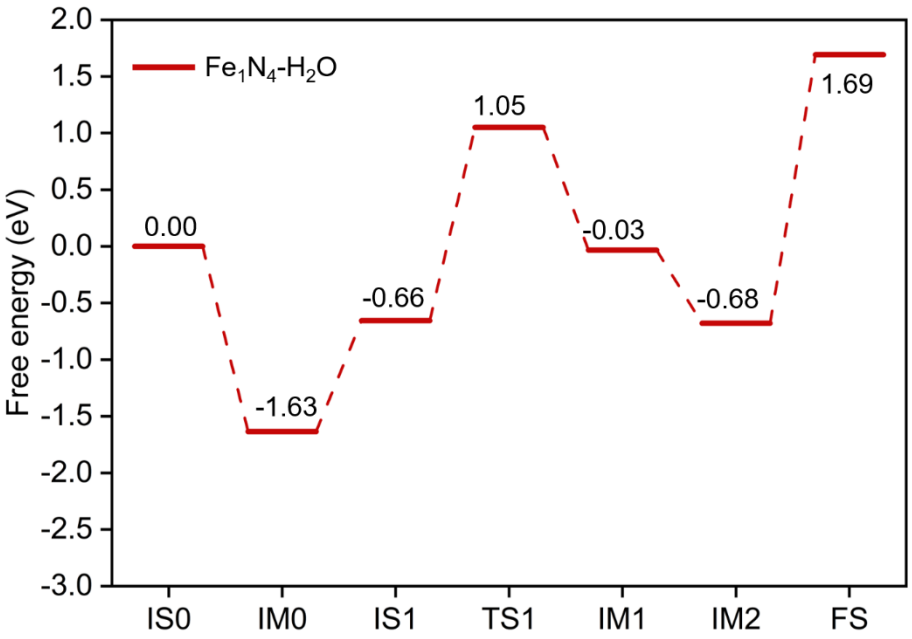

Figure S11. Free energy diagram of NO oxidation on Fe_1N_4-H_2O.

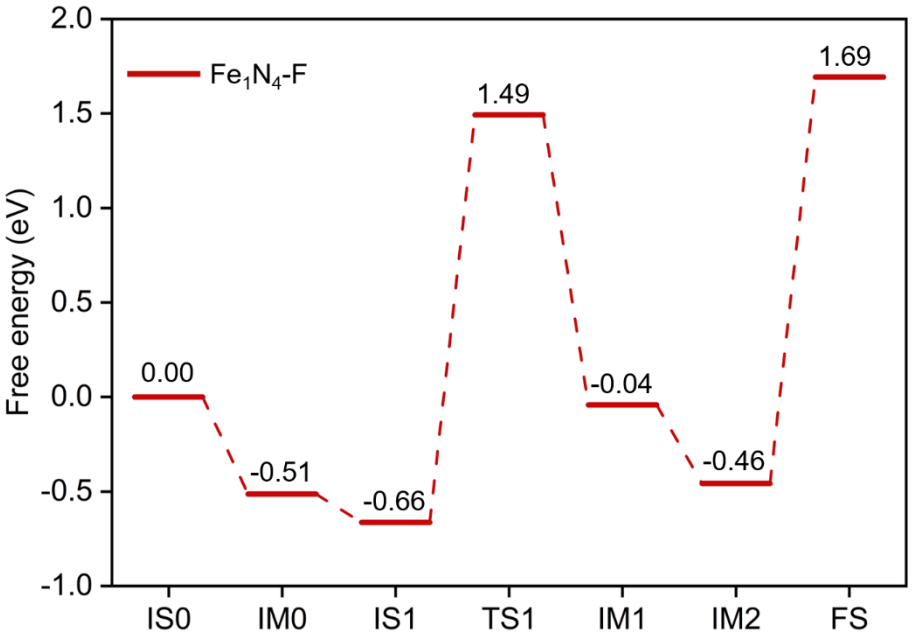

Figure S12. Free energy diagram of NO oxidation on Fe_1N_4-F.

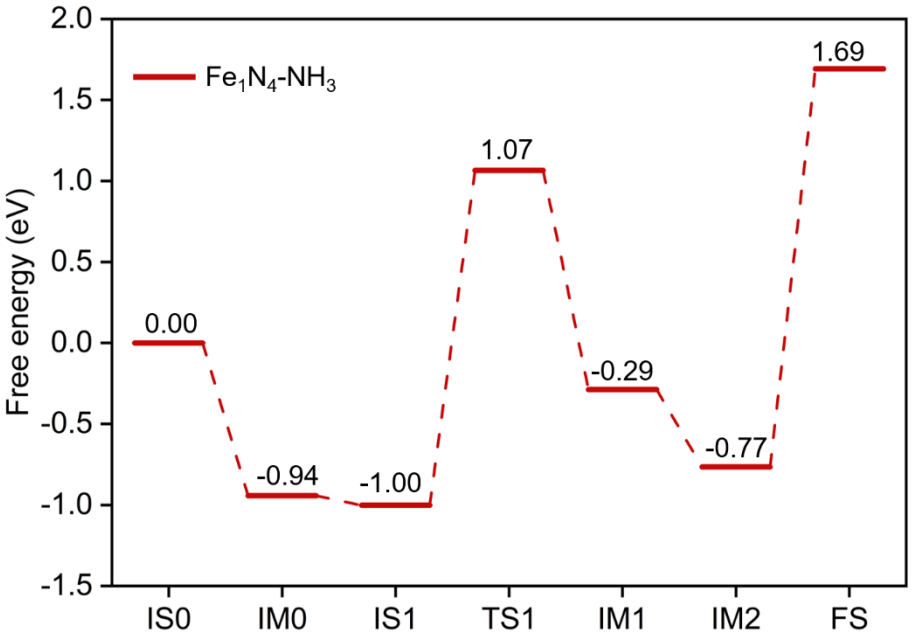

Figure S13. Free energy diagram of NO oxidation on Fe_1N_4-NH_3.

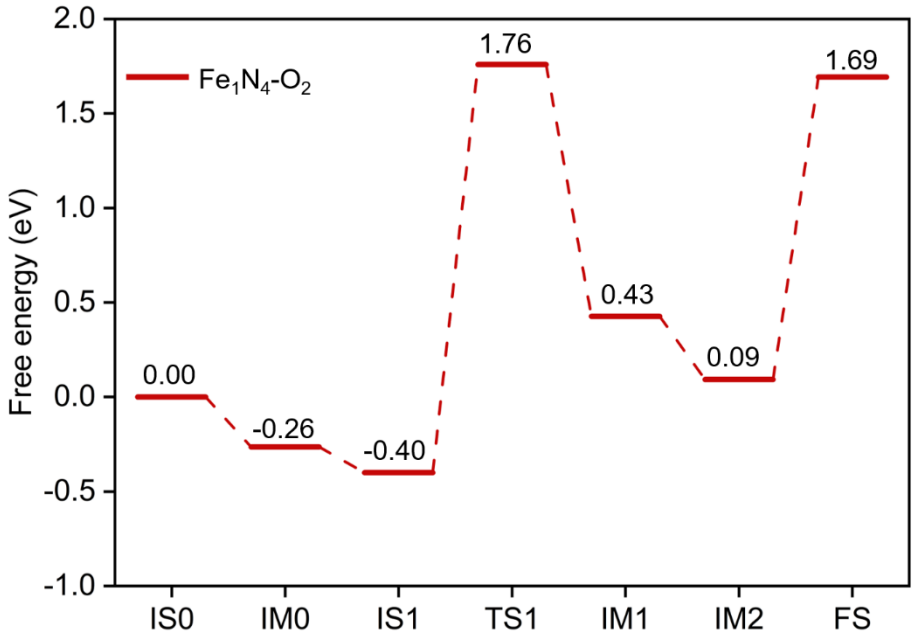

Figure S14. Free energy diagram of NO oxidation on Fe_1N_4-O_2.

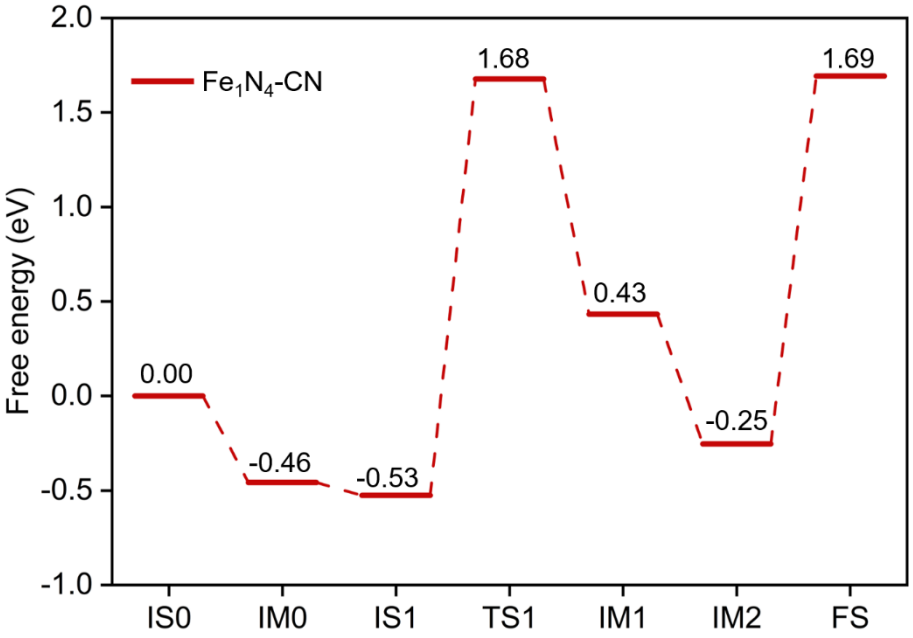

Figure S15. Free energy diagram of NO oxidation on Fe_1N_4-CN.

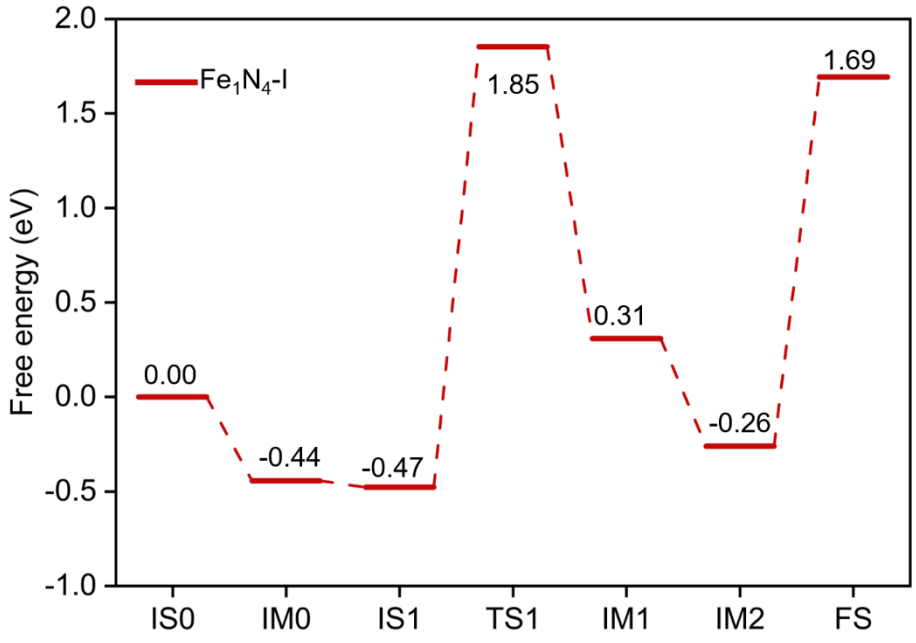

Figure S16. Free energy diagram of NO oxidation on Fe_1N_4-I.

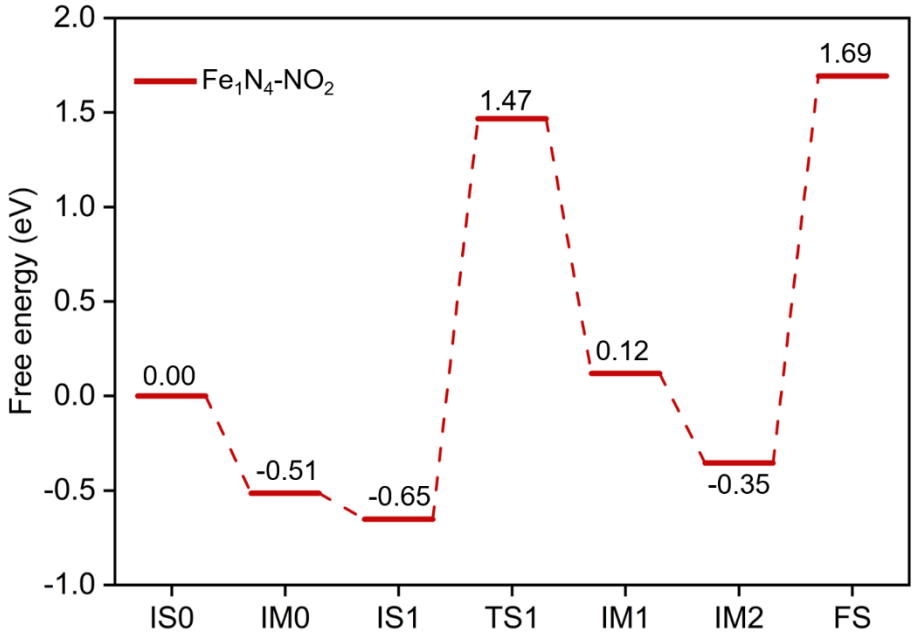

Figure S17. Free energy diagram of NO oxidation on Fe_1N_4-NO_2.

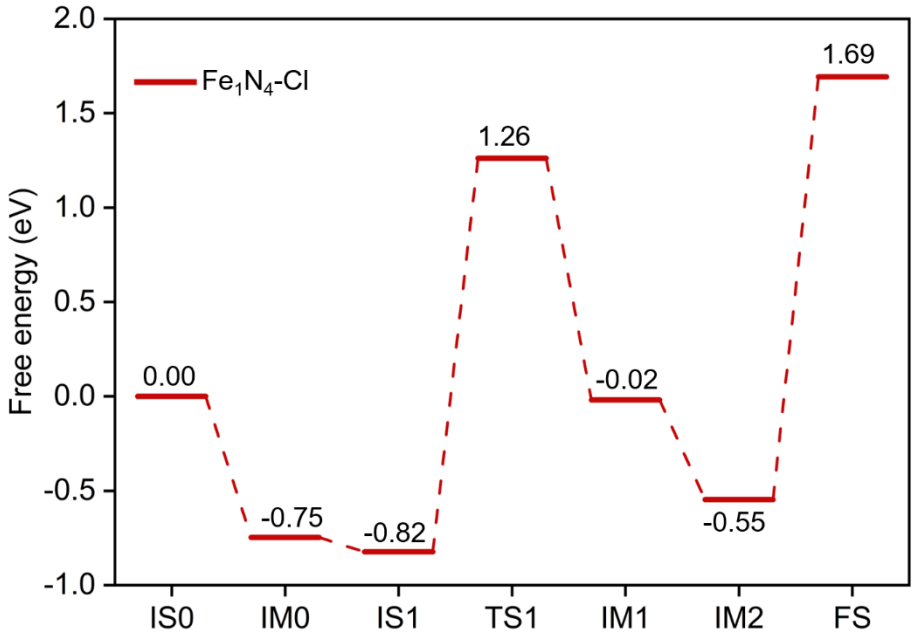

Figure S18. Free energy diagram of NO oxidation on Fe_1N_4-Cl.

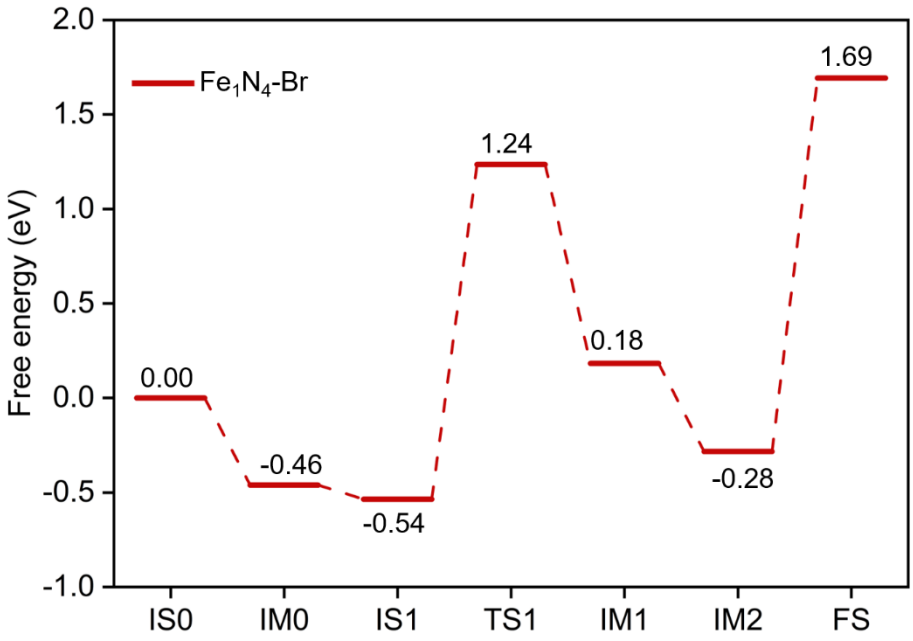

Figure S19. Free energy diagram of NO oxidation on Fe_1N_4-Br.

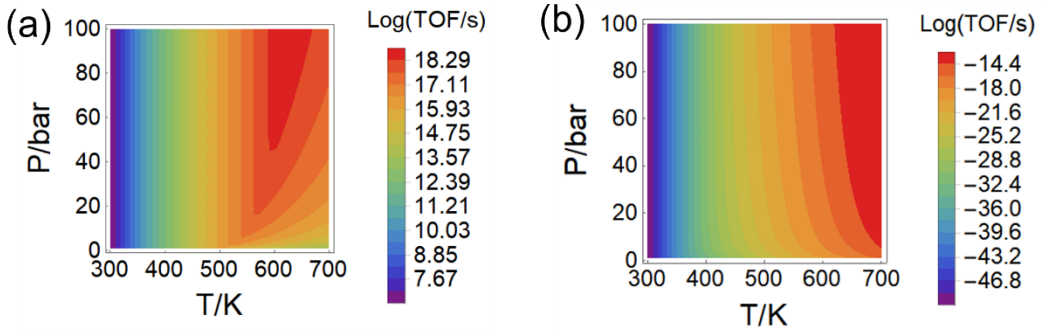

Figure S20. Microkinetic modeling analyses of the overall flue gas pressure and temperature functions in the process of catalytic oxidation NO by Fe_1N_4-Cl.

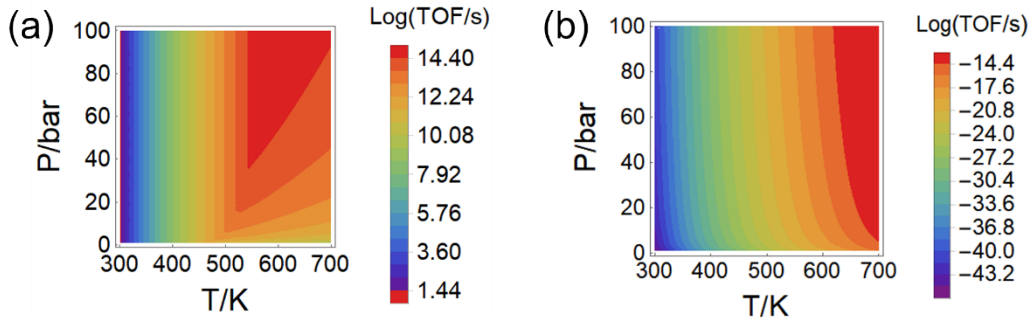

Figure S21. Microkinetic modeling analyses of the overall flue gas pressure and temperature functions in the process of catalytic oxidation NO by Fe_1N_4-Br.

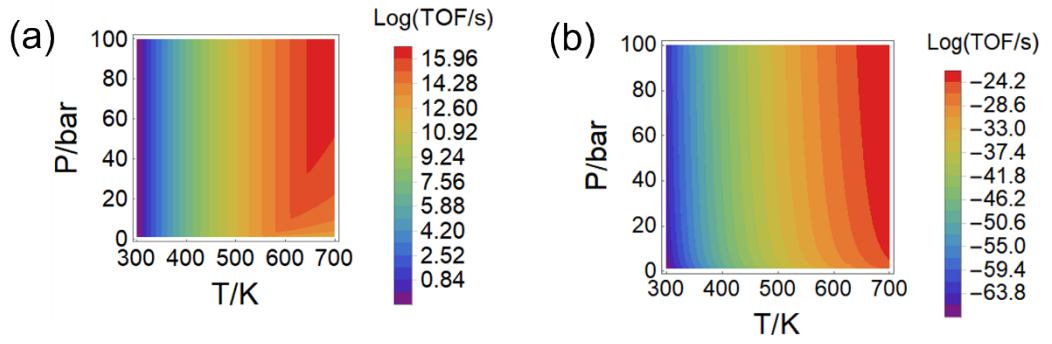

Figure S22. Microkinetic modeling analyses of the overall flue gas pressure and temperature functions in the process of catalytic oxidation NO by Fe_1N_4-I.

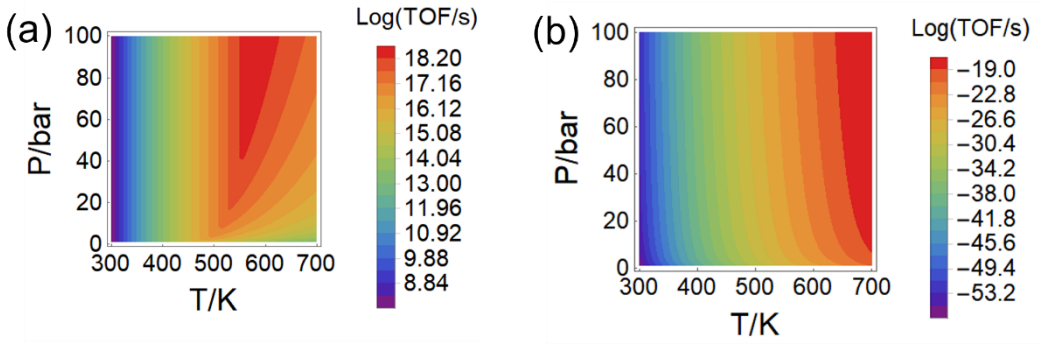

Figure S23. Microkinetic modeling analyses of the overall flue gas pressure and temperature functions in the process of catalytic oxidation NO by Fe_1N_4-NO_2.

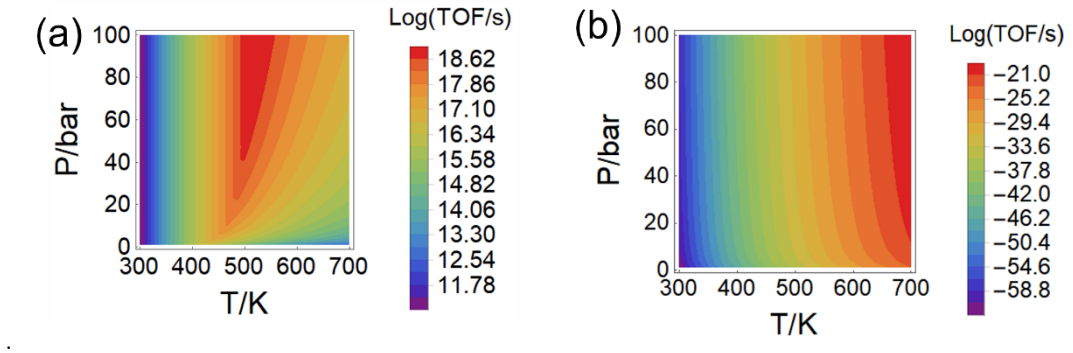

Figure S24. Microkinetic modeling analyses of the overall flue gas pressure and temperature functions in the process of catalytic oxidation NO by Fe_1N_4-H.

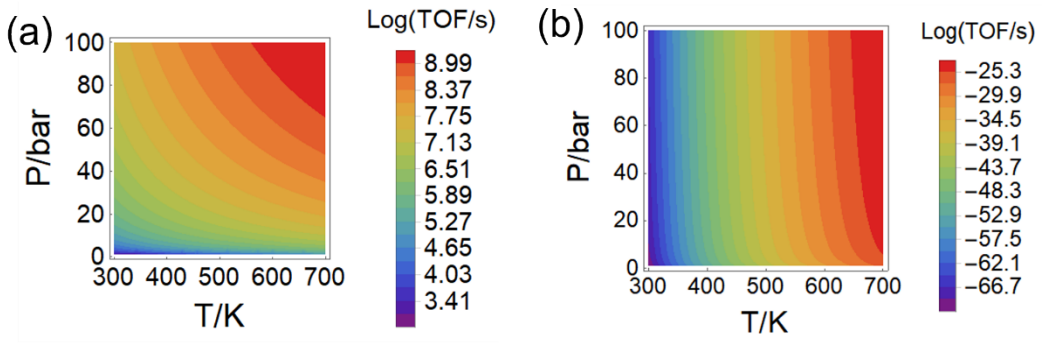

Figure S25. Microkinetic modeling analyses of the overall flue gas pressure and temperature functions in the process of catalytic oxidation NO by Fe_1N_4-O_2.

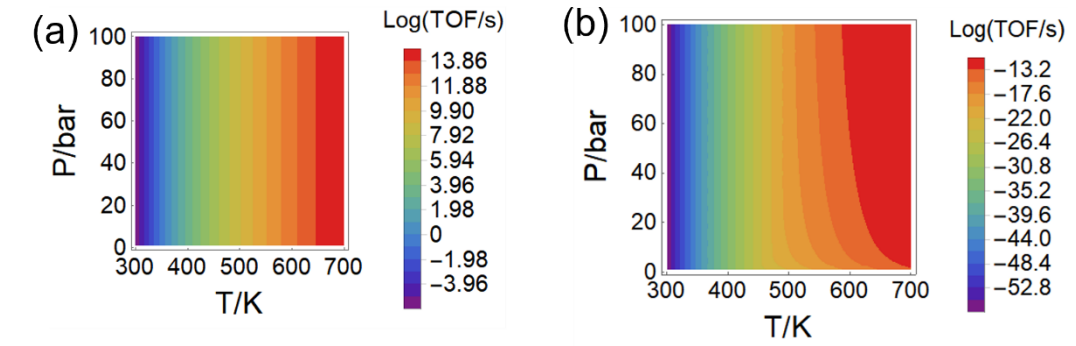

Figure S26. Microkinetic modeling analyses of the overall flue gas pressure and temperature functions in the process of catalytic oxidation NO by Fe_1N_4-NH_3.